

MSE-Type Zeolites: A Promising Catalyst for the Conversion of Ethene to Propene

Kyounghwan Lee, Seung Hyeok Cha, and Suk Bong Hong

ACS Catal., Just Accepted Manuscript • DOI: 10.1021/acscatal.6b01057 • Publication Date (Web): 13 May 2016

Downloaded from <http://pubs.acs.org> on May 16, 2016

Just Accepted

“Just Accepted” manuscripts have been peer-reviewed and accepted for publication. They are posted online prior to technical editing, formatting for publication and author proofing. The American Chemical Society provides “Just Accepted” as a free service to the research community to expedite the dissemination of scientific material as soon as possible after acceptance. “Just Accepted” manuscripts appear in full in PDF format accompanied by an HTML abstract. “Just Accepted” manuscripts have been fully peer reviewed, but should not be considered the official version of record. They are accessible to all readers and citable by the Digital Object Identifier (DOI®). “Just Accepted” is an optional service offered to authors. Therefore, the “Just Accepted” Web site may not include all articles that will be published in the journal. After a manuscript is technically edited and formatted, it will be removed from the “Just Accepted” Web site and published as an ASAP article. Note that technical editing may introduce minor changes to the manuscript text and/or graphics which could affect content, and all legal disclaimers and ethical guidelines that apply to the journal pertain. ACS cannot be held responsible for errors or consequences arising from the use of information contained in these “Just Accepted” manuscripts.



MSE-Type Zeolites: A Promising Catalyst for the Conversion of Ethene to Propene

Kyoungwan Lee, Seung Hyeok Cha, and Suk Bong Hong*

Center for Ordered Nanoporous Materials Synthesis, School of Environmental Science and Engineering, POSTECH, Pohang 790-784, Korea

ABSTRACT: The direct conversion of ethene to propene (ETP) is a potentially important route for the selective production of the latter olefin. Here we report that after some time on stream, H-UZM-35, an MSE-type large-pore zeolite, shows much better propene yield than H-SSZ-13, the best catalyst for the ETP reaction thus far. The key to this improvement is the presence of large cylindrical cages in H-UZM-35 that allows the easy formation of isopropylnaphthalene-based reaction centers for ETP catalysis, while being relatively resistant to coke formation. Mild dealumination was found to further mitigate catalyst deactivation.

KEYWORDS: ETP, propene yield, MSE structure, isopropylnaphthalene-based species, catalyst stability

There is a higher demand for polypropene than polyethylene and thus for its monomer propene (C_3^-).^{1,2} One possible approach to solve this problem is the direct conversion of ethene (C_2^-) to propene (ETP), especially when coupled with the dehydration of bioethanol, a renewable feedstock for ethene production.³ Up to date, two major types of reaction pathways have been proposed for the ETP conversion: (i) the metathesis-based ethene dimerization mechanism^{4,5} and (ii) the oligomerization-cracking one.⁶⁻⁸ Also, a number of zeolites and related microporous materials with different framework structures and compositions in their proton form, have been tested as ETP catalysts.⁹⁻¹⁴ Among them, the proton form (H-SSZ-13) of SSZ-13 (framework type CHA) shows a high propene selectivity at early time on stream (TOS), mainly due to its *cha*-cages with dimensions of $7.1 \times 7.5 \times 8.3 \text{ \AA}^3$ that allow the build-up of bulky isopropylnaphthalene-based species as reaction centers for producing propene.¹³ However, the presence of bottlenecks in this cage-based small-pore zeolite results in a high coke forming propensity and thus a fast catalyst deactivation.^{13,14}

MCM-68 (MSE) is a large-pore high-silica zeolite, first reported by Mobil researchers in 2000.¹⁵ The pore structure of this synthetic zeolite consists of one type of straight 12-ring ($6.4 \times 6.8 \text{ \AA}$) channels and two types of tortuous 10-ring (5.2×5.8 and $5.2 \times 5.2 \text{ \AA}$) channels that intersect with each other. In addition to a smaller, narrower 10-hedral ($[4^66^{10}]$) *mse*-1 cage, as a result, there is a cylindrical 24-hedral ($[4^65^86^610^4]$) *mse*-2 cage¹⁶ (Figure 1). When using the Crystal Maker software, such a unique *mse*-2 cage circumscribed by 12- and 18-rings was calculated to have approximate dimensions of $6.4 \times 6.5 \times 18.8 \text{ \AA}^3$ that are slightly more slim but much longer than those of the *cha*-cage. This led us to consider the possibility that the *mse*-2 cage could easily accommodate isopropylated naphthalene species, the ETP reaction centers, whereas its four 10-ring windows may make H-MCM-68 more resistant to coke formation than H-SSZ-13 with smaller 8-ring windows, because of their connection into the large 12-ring channels.

Zeolite MCM-68 has two related materials, i.e., YNU-2 and UZM-35.^{17,18} YNU-2 is the pure-silica analog of MCM-68 and can be obtained after the post-synthetic treatment of YNU-2P, its defect-containing precursor. The synthesis of YNU-2P includes the use of *N,N,N',N'*-tetraethylbicyclo[2.2.2]oct-7-ene-2,3:5,6-dipyrrolidinium, the original organic structure-directing agent (OSDA) yielding MCM-68,¹⁵ as well as of K^+ . In contrast, UZM-35 crystallizes as a framework Si/Al ratio similar to that (~ 9) of MCM-68 from a sodium-potassium aluminosilicate gel in the presence of dimethyldipropylammonium,¹⁸ a much simpler, commercially available OSDA. Here we report that H-UZM-35 is a promising catalyst for the ETP reaction, as we expected, apparently due to its *mse*-2 cages.



Figure 1. The 24-hedral ($[4^65^86^610^4]$) cage in MSE-type zeolites.

Figure 2 shows ethene conversion, propene selectivity and yield, and butenes yield as a function of TOS in the ETP reaction over H-SSZ-13 (Si/Al = 14), H-SAPO-34 (Si/(Si + Al + P) = 0.08), H-ZSM-5 (MFI; Si/Al = 14), and H-UZM-35 (Si/Al = 8.9 and K/Al = 0.09) measured at 673 K and 25 kPa ethene partial pressure. H-SSZ-13 and H-SAPO-34 have the same framework topology (CHA) but different compositions, and the opposite is true for all catalysts except H-SAPO-34 (Table S1). Therefore, the catalytic results in Figure 2 should illustrate the effects of both zeolite structure and composition on the ETP reaction. A notable difference (95 vs 16%) in the initial ethene conversion was found over H-SSZ-13 and H-SAPO-34. As described above, in addition, the ethene conversion over H-SSZ-13 rapidly decreases with TOS so that it becomes almost the same as the conversion over H-SAPO-34.

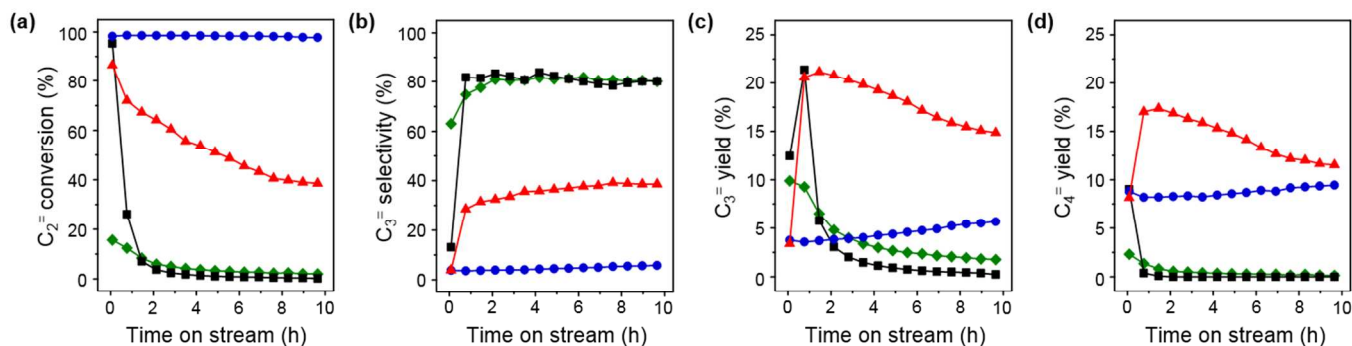


Figure 2. (a) Ethene conversion, (b) propene selectivity, (c) propene yield, and (d) butenes yield as a function of TOS in the ETP reaction over H-SSZ-13 (■), H-SAPO-34 (◆), H-ZSM-5 (●), and H-UZM-35 (▲) at 673 K and 25 kPa ethene pressure.

An unexpected observation is that the amount (27.5 vs 3.2 wt%) of organic species deposited during ETP at 673 K for 10 h on stream is exceedingly higher in H-SSZ-13 than in H-SAPO-34 (Table S1). We also found that in the case H-SSZ-13, ca. 80% of the organic is deposited during the first 1 h (Figure S1), when the catalyst is still somewhat active. The NH₃ temperature-programmed desorption (TPD) results reveal no significant differences in the acidic properties of these two CHA-type catalysts (Figure S2). However, thermal analysis indicates that the water content (6.3 wt%) in H-SSZ-13 is approximately half the content (12.3 wt%) in H-SAPO-34 (Figure S3). This suggests that the formation of isopropylated naphthalene compounds, which is highly hydrophobic in nature and is serving as organic reaction centers during ETP, should be less favorable in the more hydrophilic silicoaluminophosphate (SAPO) version of the CHA framework topology, i.e., in H-SAPO-34.

We also compared the ETP activities of H-SSZ-39 (Si/Al = 7.6) and H-SAPO-18 (Si/(Si + Al + P) = 0.05), the aluminosilicate and SAPO versions of the cage-based AEI structure,¹⁶ respectively, under the same reaction conditions (Figure S4). As for the AEI-type catalysts, a notable difference (96 vs 4 %) in the initial ethene conversion, as well as a rapid decrease in conversion over the former catalyst at early TOS, was observed. After some TOS, in consequence, both catalysts are characterized by similar catalytic behavior to each other, like their acidic properties. However, while a much higher coke content (20.9 vs 1.7 wt%) after ETP at 673 K for 10 h on stream is observed for H-SSZ-39 than for H-SAPO-18 (Table S1), the opposite holds for the water content (Figure S4). Since all these results are practically identical with those

found in H-SSZ-13 and H-SAPO-34, it is clear that the chemical composition (i.e., surface selectivity) of zeolitic catalysts has a profound effect on the ETP reaction, as observed in the *n*-hexane aromatization over Pt clusters supported on SSZ-24 and AlPO₄-5 with the same AFI topology,¹⁹ whereas this trend is substantially different from that of methanol-to-olefins (MTO) catalysis.²⁰

The ethene conversion over the channel-based medium-pore zeolite H-ZSM-5 remains almost 100% conversion during 10 h on stream. As previously reported,¹² however, its propene selectivity is poor. In fact, propane, butanes, and aromatics are the three most dominant products observed over the period of TOS studied (Figure S5). The most important result in Figure 2 is that although the initial ethene conversion (86%) over H-UZM-35 is slightly lower than that (95%) over H-SSZ-13, the extent of decrease in ethene conversion with TOS is significantly smaller over the former catalyst. Despite the fairly lower propene selectivity, therefore, the propene yield after ca. 2 h on stream becomes much higher over H-UZM-35, which led us to take into account this large-pore zeolite as a potential commercial ETP catalyst. It is worth nothing that the organic content (16.6 wt%) in H-UZM-35 after ETP at 673 K for 10 h is rather lower than that (27.5 wt%) in H-SSZ-13 (Table S1), revealing its lower coking rate. H-UZM-35 was also found to produce more butenes than H-ZSM-5, particularly than H-SSZ-13 (Figure 2). Like propene, butenes are important raw materials for the manufacture of various polymers and petrochemicals.²¹

To check whether the (partially) deactivated zeolite catalysts can be regenerated, we calcined H-SSZ-13 and H-UZM-35 after 10 h of ETP in flowing air at 823 K for 1 h and then

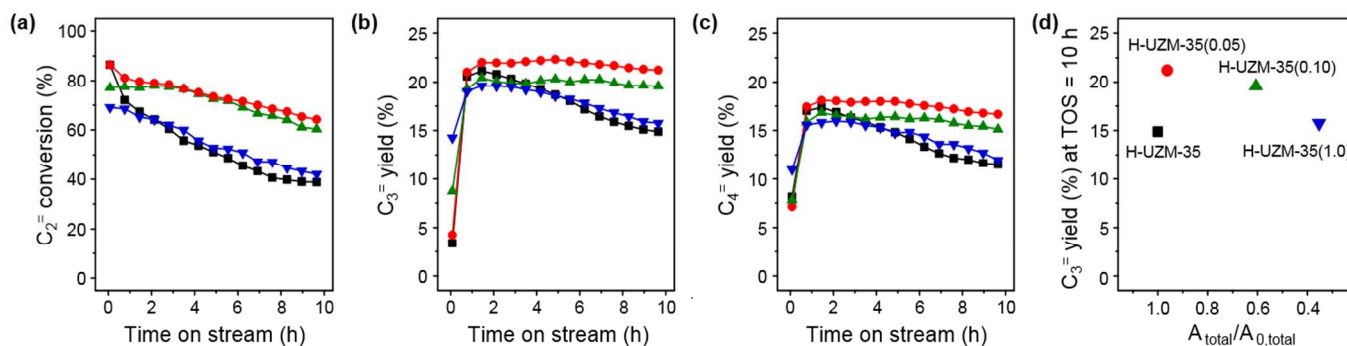


Figure 3. (a) Ethene conversion, (b) propene yield, and (c) butenes yield as a function of TOS in the ETP reaction over H-UZM-35 (■), H-UZM-35(0.05) (●), H-UZM-35(0.10) (▲), and H-UZM-35(1.0) (▼) at 673 K and 25 kPa ethene pressure. The value added in parentheses to the catalyst name is the molar concentration of HNO₃ solutions used in acid treatment. (d) Propene yield at 10 h on stream in the ETP reaction vs ratio of the NH₃ desorption peak area (A_{total}) from each dealuminated H-UZM-35 to that (A_{0,total}) from the parent H-UZM-35.

carried out the ETP reaction over the resulting materials under identical conditions. Both zeolites recovered the initial catalytic performance of their fresh form (Figure S6), suggesting that the carbonaceous deposits formed in H-SSZ-13 and H-UZM-35 are mostly light volatile soft coke. As shown in Figure 2, on the other hand, the propene yield gradually decreases with TOS. To improve this situation, we attempted to control the acidic properties of H-UZM-35 by treating with different concentrations (0.05 – 1.0 M) of HNO₃ solutions at 353 K for 4 h. Since both MCM-68 and UZM-35 can be synthesized only in a very narrow range of Si/Al ratios, in fact, acid treatment is one effective way of post-synthetically controlling the framework Si/Al ratio of these MSE-type zeolites and thus their acidity.

Three dealuminated H-UZM-35 zeolites, the bulk Si/Al ratios of which are 13, 14, and 18, respectively (Table S1), were prepared by the HNO₃ treatment of the parent H-UZM-35 with a Si/Al = 8.9 and denoted as H-UZM-35(*n*), where *n* is the molar concentration of HNO₃ solutions employed. Powder X-ray diffraction and N₂ sorption measurements reveal that their structural integrity remains intact (Table S1 and Figure S7). But NH₃ TPD shows noticeable differences in the acid

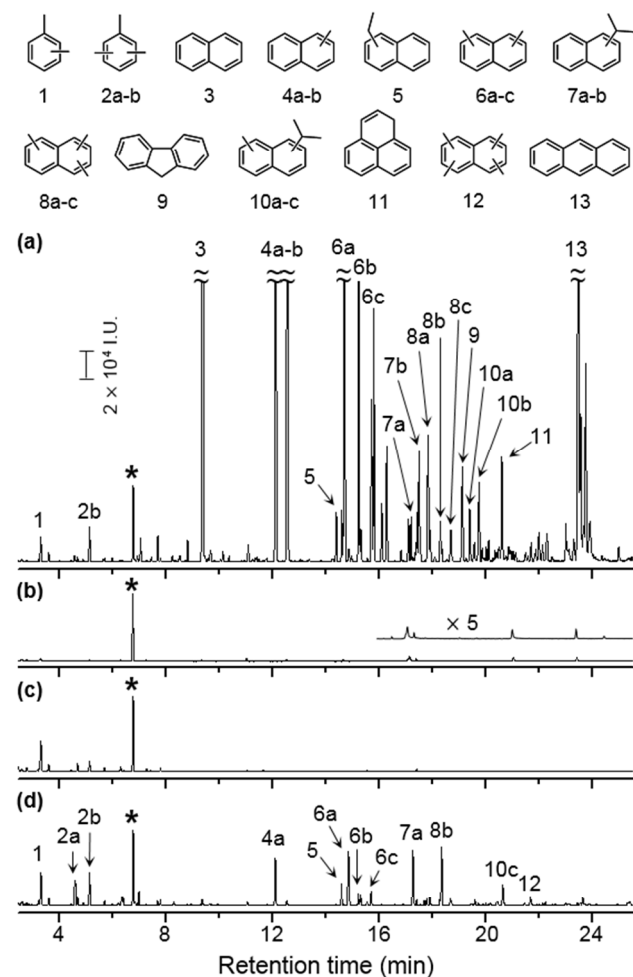


Figure 4. GC-MS total ion chromatograms of the CH₂Cl₂ extracts from (a) H-SSZ-13, (b) H-SAPO-34, (c) H-ZSM-5, and (d) H-UZM-35 after ETP at 673 K and 25 kPa ethene pressure for 30 min on stream. The structures annotated above the chromatogram are peak identifications made by comparing the mass spectra with those in the NIST database,²² and the peaks indicated by an asterisk is the mass signal of C₂Cl₆ used as an internal.

concentration (Figure S8). The ethene conversion, propene yield, and butenes yield as a function of TOS in the ETP reaction over these three dealuminated H-UZM-35 zeolites, as well as over the parent zeolite, at 673 K and 25 kPa ethene partial pressure are compared in Figure 3. A noticeable improvement in the extent of conversion decrease with TOS can be observed for H-UZM-35(0.05) and H-UZM-35(1.0), giving no noticeable decrease of yield in propene and butenes over the period of TOS studied. Because this is not the case of H-UZM-35(1.0), however, there appear to be an optimum level of acid concentration for enhancing the ETP stability of H-UZM-35.

Figure 4 shows the gas chromatography–mass spectroscopy (GC-MS) total ion chromatograms of the CH₂Cl₂ extracts from H-SSZ-13, H-SAPO-34, H-ZSM-5, and H-UZM-35 after ETP at 673 K and 25 kPa ethene pressure for 30 min on stream, when all four zeolitic catalysts are still active (Figure 2), together with the assignments of the observed peaks made by comparing their mass spectra with the NIST database.²² Trimethylbenzenes, one group of the important active intermediates involved in the hydrocarbon pool mechanism for MTO catalysis,²³ are observed in the chromatogram from H-SSZ-13. However, they are hardly detectable from H-SAPO-34, probably due to the quite low rate of formation of aromatic hydrocarbon pool species within this catalyst (Table S1 and Figure S1). This also the case of isopropyl-naphthalene (peaks 7a and 7b) and isopropylmethyl-naphthalene (peaks 10a-c) species recently reported as the active reaction centers for propene formation,¹³ which have two and 14 possible isomers, respectively (Figure S9).

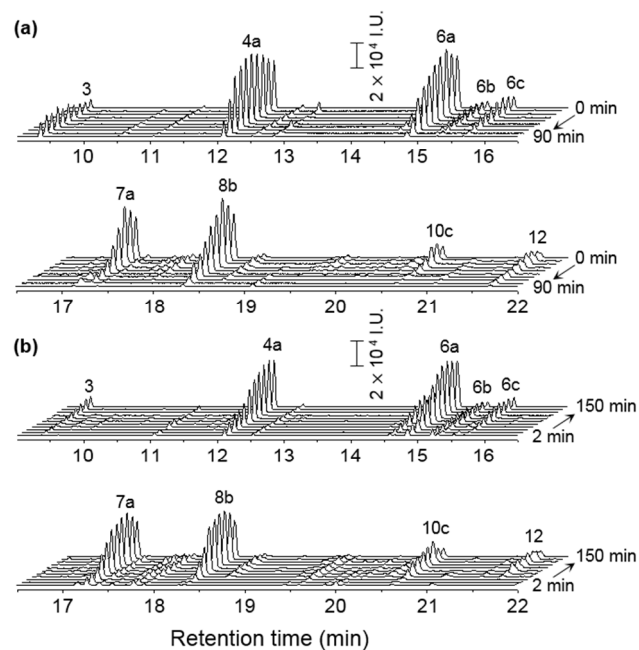


Figure 5. (a) GC-MS total ion chromatograms of the CH₂Cl₂ extracts from H-UZM-35 after ethene conversion at 673 K and 25 kPa ethene pressure for 90 min on stream followed by flushing with N₂ (30 mL min⁻¹) for 0, 1, 2, 4, 8, 10, 20, 30, 60, and 90 min (from rear to front). (b) GC-MS total ion chromatograms of the CH₂Cl₂ extracts from H-UZM-35 after ethene conversion at 673 K and 25 kPa ethene pressure for 2, 5, 10, 15, 20, 30, 50, 70, 90, 120, and 150 min on stream (from front to rear). Peak identifications are the same as those in Figure 4.

As expected from the low propene selectivity, the GC-MS signals of naphthalene-based derivatives are completely missing in the chromatogram from H-ZSM-5 with two intersecting 10-ring channels. However, they are clearly resolved in the chromatogram from H-UZM-35 containing *mse-2* cages. Of particular interest is that the type and concentration of such bicyclic compounds found in this large-pore zeolite is significantly different from those in H-SSZ-13 with the slightly more rotund *cha*-cages. This indicates that the formation of active aromatic hydrocarbon pool species during ETP can be greatly affected not only by the composition of zeolitic catalysts, but also by the size and shape of their cages, if present.

To clarify the role of isopropyl-naphthalene (*ip*NPTH) and isopropylmethyl-naphthalene (*ipm*NPTH) derivatives during ETP, we reacted ethene over H-UZM-35 at 673 K for 90 min on stream, when the maximum propene yield is obtained (Figure 2), divided the resulting catalyst into a series of batches, and then flushed them in a pure N₂ stream (30 mL min⁻¹) at the same temperature for times up to 90 min. As shown in Figure 5, the two peaks 7a and 10c, which represent the *ip*NPTH and *ipm*NPTH species, respectively, increase in intensity at the beginning of the flushing time, level off, and then decrease after 4 min. We also monitored their generation as a function of TOS in H-UZM-35 during ETP at the same reaction temperature (Figure 5). Both peaks were found to continuously increase until 90 min on stream. The same trend can be observed for peaks 3 and 4a due to naphthalene and methylnaphthalenes that are the products of *ip*NPTH and *ipm*NPTH decompositions, respectively, leading to propene formation. Therefore, it is most likely that *ip*NPTH and *ipm*NPTH species are the most important active intermediates of the ETP reaction over H-UZM-35. This matches well with the rapid increase in organic content deposit on this large-pore zeolite at early TOS (Figure S1), as well as in propene yield (Figure 2).

Other major groups of aromatic hydrocarbon compounds clearly observed in Figure 5 include the polymethylnaphthalenes with two, three, and four methyl groups represented by peaks 6a-c, 8b, and 12, respectively. We should note here that while the generation and consumption patterns of these aromatic species are essentially the same as those of *ip*NPTH and *ipm*NPTH, such naphthalene-based derivatives are known as active organic reaction centers for MTO catalysis.²⁴ Therefore, we cannot rule out the possibility that polymethylnaphthalenes could also play such a role during ETP. To elucidate this, further study is currently underway in our laboratory.

Finally, we calculated the strain energies of two *ip*NPTH isomers (i.e., 1-isopropyl-naphthalene (1-*ip*NPTH) and 2-isopropyl-naphthalene (2-*ip*NPTH)) and two *ipm*NPTH isomers in SSZ-13 and UZM-35 to gain further insights into the intrazeolitic formation of naphthalene-based intermediates during ETP (Figure S10). Here we selected 1-isopropyl-3-methylnaphthalene (1-*ip-3-m*NPTH) and 2-isopropyl-7-methylnaphthalene (2-*ip-7-m*NPTH), fattest and most slim among the 14 possible *ipm*NPTH isomers, respectively (Table S2 and Figure S9), as two representative isomers to save the computational cost. Zero or small differences (0 and 7 kJ mol⁻¹, respectively) in the strain energy are observed for these two pairs of naphthalene derivatives when embedded in SSZ-13. As shown in Figure S10, however, their strain energy differences become much larger (24 and 145 kJ mol⁻¹, respectively) upon encapsulation within the *mse-2* cages in UZM-35. These

results allowed us to assign the GC-MS peak 7a in Figure 4 to 2-*ip*NPTH. Similarly, peak 10c can be tentatively assigned to the most slim 2-*ip-7-m*NPTH isomer. If such is the case, peak 7b could then be attributed to the fatter 1-*ip*NPTH isomer. Therefore, we think that the type of active aromatic hydrocarbon pool species formed during ETP over cage-containing zeolite catalysts can differ notably according to the size and shape of zeolite cages.

In summary, we have demonstrated that H-UZM-35 with the MSE topology outperforms any of the earlier zeolitic catalysts tested in the ETP reaction. A combination of GC-MS and DFT calculation results reveals that the superior ETP performance of this large-pore zeolite comes from its unique cylindrical cages in which ethene can be effectively converted to isopropyl-naphthalene-based hydrocarbon species, playing a central role as reaction centers in propene formation. Apart from the relatively lower coke forming tendency compared to H-SSZ-13 with small 8-ring windows, the ETP stability of H-UZM-35 can be further improved by mild dealumination.

ASSOCIATED CONTENT

Supporting Information. Experimental section, characterization data, and additional results. This material is available free of charge via the Internet at <http://pubs.acs.org>.

AUTHOR INFORMATION

Corresponding Author

*S.B.H: e-mail, sbhong@postech.ac.kr

Notes

The authors have applied for a patent based on the reaction reported in this paper.

ACKNOWLEDGMENT

This work was supported the National Creative Research Initiative Program (2012R1A3A2048833) through the National Research Foundation of Korea.

REFERENCES

- (1) Plotkin, J. *Catal. Today* **2005**, 106, 10-14.
- (2) Tullo, A. H. *Chem. Eng. News* **2007**, 85, 27-29.
- (3) Zhang, M.; Yu, Y. *Ind. Eng. Chem. Res.* **2013**, 52, 9505-9514.
- (4) Taoufik, M.; Roux, E. L.; Thivolle-Cazat, J.; Basset, J.-M. *Angew. Chem. Int. Ed.* **2007**, 46, 7202-7205.
- (5) Mazoyer, E.; Szeto, K. C.; Merle, N.; Thivolle-Cazat, J.; Boyron, O.; Basset, J.-M.; Nicholas, C. P.; Taoufik, M. *J. Mol. Catal. A* **2014**, 385, 125-132.
- (6) Quann, R. J.; Green, L. A.; Tabak, S. A.; Krambeck, F. J. *Ind. Eng. Chem. Res.* **1988**, 27, 565-570.
- (7) Ding, X.; Li, C.; Yang, C. *Energy Fuels* **2010**, 24, 3760-3763.
- (8) Chen, C.-J.; Rangarajan, S.; Hill, I. M.; Bhan, A. *ACS Catal.* **2014**, 4, 2319-2327.
- (9) Oikawa, H.; Shibata, Y.; Inazu, K.; Iwase, Y.; Murai, K.; Hyodo, S.; Kobayashi, G.; Baba, T. *Appl. Catal. A* **2006**, 312, 181-185.
- (10) Iwase, Y.; Motokura, K.; Koyama, T.; Baba, T. *Phys. Chem. Chem. Phys.* **2009**, 11, 9268-9277.
- (11) Lin, B.; Zhang, Q.; Wang, Y. *Ind. Eng. Chem. Res.* **2009**, 48, 10788-10795.
- (12) Koyama, T.; Hayashi, Y.; Horie, H.; Kawachi, S.; Matsumoto, A.; Iwase, Y.; Sakamoto, Y.; Miyaji, A.; Motokura, K.; Baba, T. *Phys. Chem. Chem. Phys.* **2010**, 12, 2541-2554.
- (13) Dai, W.; Sun, X.; Tang, B.; Wu, G.; Li, L.; Guan, N.; Hunger, M. *J. Catal.* **2014**, 314, 10-20.
- (14) Epelde, E.; Ibañez, M.; Aguayo, A. T.; Gayubo, A. G.; Bilbao, J.; Castaño, P. *Microporous Mesoporous Mater.* **2014**, 195, 284-293.

1 (15) Calabro, D. C.; Cheng, J. C.; Crane, R. A.; Kresge, C. T.;
2 Dhingra, S. S.; Steckel, M. A.; Stern, D. L.; Weston, S. C. U.S. Patent
3 6049018, 2000.

4 (16) Baerlocher, Ch.; McCusker, L. B. Database of Zeolite Struc-
5 tures, <http://www.iza-structure.org/databases/>.

6 (17) Koyama, Y.; Ikeda, T.; Tatsumi, T.; Kubota, K. *Angew. Chem.*
7 *Int. Ed.* **2008**, 47, 1042-1046.

8 (18) Moscoso, J. G.; Jan, D.-Y. U.S. Patent 7922997, 2011.

9 (19) Mielczarski, E.; Hong, S. B.; Davis, M. E. *J. Catal.* **1992**, 134,
10 370-372.

(20) Olsbye, U.; Svelle, S.; Bjørgen, M.; Beato, P.; Janssens, T. V.
11 W.; Joensen, F.; Bordiga, S.; Lillerud, K. P. *Angew. Chem. Int. Ed.*
12 **2012**, 51, 5810-5831.

13 (21) Bender, M. *ChemBioEng Rev.* **2014**, 1, 136-147.

14 (22) NIST Chemistry Web book, [http://webbook.nist.gov/chemis-](http://webbook.nist.gov/chemistry/)
15 [try/](http://webbook.nist.gov/chemistry/).

16 (23) Arstad, B.; Nicholas, J. B.; Haw, J. F. *J. Am. Chem. Soc.* **2004**,
17 126, 2991-3001.

18 (24) Song, W.; Fu, H.; Haw, J. F. *J. Phys. Chem. B* **2001**, 105,
19 12839-12843.

SYNOPSIS TOC

MSE-Type Zeolites: A Promising Catalyst for the Conversion of Ethene to Propene

Kyoungwan Lee, Seung Hyeok Cha, and Suk Bong Hong*

